

THEORETICAL DIRECTIONAL AND MODULATED RATES FOR DIRECT SUSY DARK MATTER DETECTION

J. D. Vergados^{(1),(2)*}

⁽¹⁾ *Theoretical Physics Division, University of Ioannina, Ioannina, Gr 451 10, Greece.*

⁽²⁾ *Institute of Theoretical Physics, University of Tuebingen, Tuebingen, Germany.*

Abstract

Exotic dark matter together with the vacuum energy (cosmological constant) seem to dominate in the flat Universe. Thus direct dark matter detection is central to particle physics and cosmology. Supersymmetry provides a natural dark matter candidate, the lightest supersymmetric particle (LSP). It is possible to obtain detectable rates, but realistically they are expected to be much lower than the present experimental goals. So one should exploit two characteristic signatures of the reaction, namely the modulation effect and the correlation with the sun's motion in directional experiments. In standard non directional experiments the modulation is small, less than two per cent. In the case of the directional experiments, the main subject of this paper, we find two novel features, which are essentially independent of the SUSY model employed, namely: 1) The forward-backward asymmetry, with respect to the sun's direction of motion, is very large and 2) The modulation observed in a plane perpendicular to the sun's motion can be higher than 20 per cent and is direction dependent.

PACS numbers:95.35.+d, 12.60.Jv

*vergados@cc.uoi.gr

I. INTRODUCTION

The combined MAXIMA-1 [1], BOOMERANG [2], DASI [3] and COBE/DMR Cosmic Microwave Background (CMB) observations [4] imply that the Universe is flat [5], $\Omega = 1.11 \pm 0.07$, while the baryonic component is very small $\Omega_b h^2 = 0.032^{+0.009}_{-0.008}$. Furthermore exotic dark matter has become necessary in order to close the Universe. In fact about a decade ago the COBE data [4] suggested that CDM (Cold Dark Matter) dominates the Universe, Ω_{CDM} being at least 60% [6]. Subsequent evidence from two different teams, the High-z Supernova Search Team [7] and the Supernova Cosmology Project [8] , [9] changed this view suggesting that the Universe may be dominated by the cosmological constant Λ or dark energy. In other words one roughly finds a baryonic component $\Omega_B = 0.1$ along with the exotic components $\Omega_{CDM} = 0.3$ and $\Omega_\Lambda = 0.6$. In a more detailed recent Λ CDM analysis by Primack [10] (see also the analysis by Einasto [11]) we find $h = 0.72 \pm 0.08$, $\Omega_b = 0.040 \pm 0.002$, and $\Omega_m = \Omega_{CDM} = 0.33 \pm 0.035$ (from cluster baryons etc), $0.4| \pm 0.2$ (from cluster evolution) and 0.34 ± 0.1 (from $Ly\alpha$ forest $P(k)$), while $\Omega_{HDM} \leq 0.05$ and $\Omega_\Lambda = 0.73 \pm 0.08$. In other words $\Omega_m \approx 3/4 \Omega_\Lambda$. Since the non exotic component cannot exceed 40% of the CDM [12], there is room for the exotic WIMP's (Weakly Interacting Massive Particles). In fact the DAMA experiment [13] has claimed the observation of one signal in direct detection of a WIMP, which with better statistics has subsequently been interpreted as a modulation signal [14].

Supersymmetry naturally provides candidates for the dark matter constituents [15]-[18]. In the most favored scenario of supersymmetry the LSP can be simply described as a Majorana fermion, a linear combination of the neutral components of the gauginos and Higgsinos [15]- [22]. The main ingredients of the SUSY input are summarized in the next section. The essential features of the LSP-nucleus cross-section are discussed in sect. 3. The basic formulas for the event rates, in the case of Gaussian models as well as those due caustic rings, are given in sect. 4. The results obtained both for the non directional as well as the directional experiments are discussed in sect. 5. Finally in sect. 6 we present our conclusions.

II. THE ESSENTIAL THEORETICAL INGREDIENTS OF DIRECT DETECTION.

It is well known that there exists indirect evidence for a halo of dark matter from the observed rotational curves. It is, however, essential to directly detect [15]- [26] such matter, since this, among other things, will also unravel the nature of the constituents of dark matter. The possibility of detection depends on the nature of such constituents. Here we will assume that such a constituent is the LSP. Since this particle is expected to be very massive, $m_\chi \geq 30\text{GeV}$, and extremely non relativistic with average kinetic energy $T \approx 50\text{KeV}(m_\chi/100\text{GeV})$, it can be directly detected [15]- [26] mainly via the recoiling of a nucleus (A,Z) in elastic scattering. The event rate for such a process can be computed from the following ingredients:

- 1) An effective Lagrangian at the elementary particle (quark) level obtained in the framework of supersymmetry as described , e.g., in Refs [22,23].
- 2) A well defined procedure for transforming the amplitude obtained from the previous effective Lagrangian from the quark to the nucleon level, i.e. a quark model for the nucleon. This step is not trivial since the obtained results depend crucially on the content of the nucleon in quarks other than u and d. This is particularly true for the scalar couplings, which are proportional to the quark masses [27]– [30] as well as the isoscalar axial coupling.
- 3) Compute the relevant nuclear matrix elements [31]– [33]. using as reliable as possible many body nuclear wave functions. Fortunately in the case of the scalar coupling, which is viewed as the most important, the situation is a bit simpler, since then one needs only the nuclear form factor.

Since the obtained rates are very low, one would like to be able to exploit the modulation of the event rates due to the earth's revolution around the sun [34,35] [36]– [39]. In order to accomplish this one adopts a folding procedure, i.e one has to assume some velocity distribution [34,40], [37,39], [41]- [43] for the LSP. One also would like to exploit the signatures expected to show up in directional experiments, by observing the nucleus in a certain direction. Since the sun is moving with relatively high velocity with respect to the center of the galaxy one expects strong correlation of such observations with the

motion of the sun [19,44]. On top of this one expects in addition to see a more interesting pattern of modulation.

The calculation of this cross section has become pretty standard. One starts with representative input in the restricted SUSY parameter space as described in the literature [20,22] (see also Arnowitt and Dutta [24]). We have adopted a similar procedure, which has previously described [20] and will not be repeated here. In the above procedure the most important constraints on the SUSY parameter space come from [24,20]:

- 1.) The LSP relic abundance which must satisfy the cosmological constrain:

$$0.09 \leq \Omega_{LSP} h^2 \leq 0.22 \quad (1)$$

2.) The Higgs mass bound. The bound is obtained from the recent experiments CDF experiment [45] and, especially the LEP2 signal [46], [47] $m_h = 115^{1.3}_{-0.9} \text{ GeV}$, in SUSY cannot unambiguously attributed to a definite mass eigenstate. Furthermore in the LSP-nucleus scattering both physical scalar eigenstates contribute (the surviving pseudoscalar does not lead to coherence). The correct prediction for the Higgs mass, however, is essential, since it imposes important constraints on the allowed parameter space [48], [49].

- 3.) The $b \rightarrow s \gamma$ limit and the bound on the anomalous magnetic moment of the muon, see, e.g., recent work and references therein [25].
- 4.) The need to will ourselves to LSP-nucleon cross sections for the scalar coupling, which gives detectable rates

$$4 \times 10^{-7} \text{ pb} \leq \sigma_{\text{scalar}}^{\text{nucleon}} \leq 2 \times 10^{-5} \text{ pb} \quad (2)$$

This is because above this range the direct observation of LSP should have occurred in the experimental searches so far and below this it is unobservable. We should remember, however, that the event rate does not depend only on the nucleon cross section, but on other parameters also, mainly on the LSP mass and the nucleus used in target. The condition on the nucleon cross section imposes the most severe constraints on the acceptable parameter space. In particular in our model [20] as well as in other models [51,25] it restricts $\tan\beta$ to values $\tan\beta \simeq 50$.

III. THE LSP-NUCLEUS EXPRESSIONS DIFFERENTIAL CROSS SECTION .

The expressions for this cross-section are well known. We will, however, summarize the main ingredients here for the reader's convenience and in order to establish notation.

To begin with the effective Lagrangian describing the LSP-nucleus cross section can be conveniently put in a form familiar from weak interactions: [23]

$$L_{eff} = -\frac{G_F}{\sqrt{2}} \{ (\bar{\chi}_1 \gamma^\lambda \gamma_5 \chi_1) J_\lambda + (\bar{\chi}_1 \chi_1) J \} \quad (3)$$

where

$$J_\lambda = \bar{N} \gamma_\lambda (f_V^0 + f_V^1 \tau_3 + f_A^0 \gamma_5 + f_A^1 \gamma_5 \tau_3) N \quad , \quad J = \bar{N} (f_s^0 + f_s^1 \tau_3) N \quad (4)$$

We have neglected the uninteresting pseudoscalar and tensor currents. Note that, due to the Majorana nature of the LSP, $\bar{\chi}_1 \gamma^\lambda \chi_1 = 0$ (identically).

With the above ingredients the differential cross section can be cast in the form [19,36,37]

$$d\sigma(u, v) = \frac{du}{2(\mu_r b v)^2} [(\bar{\Sigma}_S + \bar{\Sigma}_V \frac{v^2}{c^2}) F^2(u) + \bar{\Sigma}_{spin} F_{11}(u)] \quad (5)$$

$$\bar{\Sigma}_S = \sigma_0 \left(\frac{\mu_r(A)}{\mu_r(N)} \right)^2 \{ A^2 [(f_S^0 - f_S^1 \frac{A - 2Z}{A})^2] \} \simeq \sigma_{p,\chi^0}^S A^2 \left(\frac{\mu_r(A)}{\mu_r(N)} \right)^2 \quad (6)$$

$$\bar{\Sigma}_{spin} = \sigma_{p,\chi^0}^{spin} \zeta_{spin} \quad , \quad \zeta_{spin} = \frac{(\mu_r(A)/\mu_r(N))^2}{3(1 + \frac{f_A^0}{f_A^1})^2} S(u) \quad (7)$$

$$S(u) = [(\frac{f_A^0}{f_A^1} \Omega_0(0))^2 \frac{F_{00}(u)}{F_{11}(u)} + 2 \frac{f_A^0}{f_A^1} \Omega_0(0) \Omega_1(0) \frac{F_{01}(u)}{F_{11}(u)} + \Omega_1(0))^2] \quad (8)$$

$$\bar{\Sigma}_V = \sigma_{p,\chi^0}^V \zeta_V \quad (9)$$

$$\zeta_V = \frac{(\mu_r(A)/\mu_r(N))^2}{(1 + \frac{f_V^1}{f_V^0})^2} A^2 \left(1 - \frac{f_V^1}{f_V^0} \frac{A - 2Z}{A} \right)^2 \left[\left(\frac{v_0}{c} \right)^2 \left[1 - \frac{1}{(2\mu_r b)^2} \frac{2\eta + 1}{(1 + \eta)^2} \frac{\langle 2u \rangle}{\langle v^2 \rangle} \right] \right] \quad (10)$$

σ_{p,χ^0}^i = proton cross-section, $i = S, spin, V$ given by:

$\sigma_{p,\chi^0}^S = \sigma_0 (f_S^0)^2 (\frac{\mu_r(N)}{m_N})^2$ (scalar) , (the isovector scalar is negligible, mainly since the heavy quarks dominate [27]–[30], i.e. $\sigma_p^S = \sigma_n^S$)

$\sigma_{p,\chi^0}^{spin} = \sigma_0 3 (f_A^0 + f_A^1)^2 (\frac{\mu_r(N)}{m_N})^2$ (spin) , $\sigma_{p,\chi^0}^V = \sigma_0 (f_V^0 + f_V^1)^2 (\frac{\mu_r(N)}{m_N})^2$ (vector)

where m_N is the nucleon mass, $\eta = m_x/m_N A$, and $\mu_r(A)$ is the LSP-nucleus reduced mass, $\mu_r(N)$ is the LSP-nucleon reduced mass and

$$\sigma_0 = \frac{1}{2\pi} (G_F m_N)^2 \simeq 0.77 \times 10^{-38} \text{ cm}^2 \quad (11)$$

$$Q = Q_0 u \quad , \quad Q_0 = \frac{1}{A m_N b^2} = 4.1 \times 10^4 A^{-4/3} \text{ KeV} \quad (12)$$

where Q is the energy transfer to the nucleus and $F(u)$ is the nuclear form factor and $F_{11}(u)$ is the isovector spin response factor. $S(u)$ is essentially independent of u . It depends crucially on the static spin matrix elements and the ratio of the elementary isoscalar to isovector amplitudes [33].

In the present paper we will consider both the coherent mode as well as the spin mode, but we will not focus on the nucleon cross section. For the scalar interaction we will use a form factor obtained as discussed in our earlier work. We will also consider the spin contribution, which is expected to be more important in the case of the light targets. For a discussion of the spin matrix elements we refer the reader to the literature (see Divari et al [33,50].) We only mention here that the spin matrix elements are the largest and the most accurately calculated for the $A = 19$ system. The static spin values, however, affect the quantity $\bar{\Sigma}_{spin}$, which affects the expected rate, but it is not the main subject of the present work. What is most relevant here is the spin response function $F_{11}(u)$. For the light nuclei it was taken from our earlier work [33] and for the ^{127}I target it was obtained from the calculation of Ressel *et al* [31].

The vector contribution, which, due to the Majorana nature of the LSP, is only a relativistic correction and, at present, below the level of the planned experiments, can safely be neglected.

IV. EXPRESSIONS FOR THE RATES.

The non-directional event rate is given by:

$$R = R_{non-dir} = \frac{dN}{dt} = \frac{\rho(0)}{m_\chi} \frac{m}{Am_N} \sigma(u, v) |v| \quad (13)$$

Where $\rho(0) = 0.3 \text{GeV/cm}^3$ is the LSP density in our vicinity and m is the detector mass. The differential non-directional rate can be written as

$$dR = dR_{non-dir} = \frac{\rho(0)}{m_\chi} \frac{m}{Am_N} d\sigma(u, v) |v| \quad (14)$$

where $d\sigma(u, v)$ was given above.

The directional differential rate [19], [39] in the direction \hat{e} is given by :

$$dR_{dir} = \frac{\rho(0)}{m_\chi} \frac{m}{Am_N} \mathbf{v} \cdot \hat{e} H \mathbf{v} \cdot \hat{e} \frac{1}{2\pi} d\sigma(u, v) \quad (15)$$

where H the Heaviside step function. The factor of $1/2\pi$ is introduced, since the differential cross section of the last equation is the same with that entering the non-directional rate, i.e. after an integration over the azimuthal angle around the nuclear momentum has been performed. In other words, crudely speaking, $1/(2\pi)$ is the suppression factor we expect in the directional rate compared to the usual one. The precise suppression factor depends, of course, on the direction of observation. The mean value of the non-directional event rate of Eq. (14), is obtained by convoluting the above expressions with the LSP velocity distribution $f(v, v_E)$ with respect to the Earth, which moves with velocity v_E relative to the sun (see below), i.e. is given by:

$$\left\langle \frac{dR}{du} \right\rangle = \frac{\rho(0)}{m_\chi} \frac{m}{Am_N} \int f(\mathbf{v}, \mathbf{v}_E) |\mathbf{v}| \frac{d\sigma(u, v)}{du} d^3 \mathbf{v} \quad (16)$$

The above expression can be more conveniently written as

$$\left\langle \frac{dR}{du} \right\rangle = \frac{\rho(0)}{m_\chi} \frac{m}{Am_N} \sqrt{\langle v^2 \rangle} \left\langle \frac{d\Sigma}{du} \right\rangle, \quad \left\langle \frac{d\Sigma}{du} \right\rangle = \int \frac{|\mathbf{v}|}{\sqrt{\langle v^2 \rangle}} f(\mathbf{v}, \mathbf{v}_E) \frac{d\sigma(u, v)}{du} d^3 \mathbf{v} \quad (17)$$

Now we perform the needed integrations. First over the velocity distribution ranging from $av_0\sqrt{u}$, where $a = [\sqrt{2}mu_r b v_0 b]^{-1}$ and b the nuclear (harmonic oscillator) length parameter, to the maximum escape velocity v_m . Second over the energy transfer u

ranging from u_{min} dictated by the detector energy cutoff to $u_{max} = (v_m/(v_0 a))^2$. Thus we get:

$$R = \bar{R} t [1 + h(a, Q_{min}) \cos \alpha] \quad (18)$$

where t is the total rate in the absence of modulation, α is the phase of the Earth ($\alpha = 0$ around June 2nd) and Q_{min} is the energy transfer cutoff imposed by the detector. In the above expressions \bar{R} is the rate obtained in the conventional approach [23] by neglecting the folding with the LSP velocity and the momentum transfer dependence of the differential cross section, i.e. by

$$\bar{R} = \frac{\rho(0)}{m_\chi} \frac{m}{Am_N} \sqrt{\langle v^2 \rangle} [\bar{\Sigma}_S + \bar{\Sigma}_{spin} + \frac{\langle v^2 \rangle}{c^2} \bar{\Sigma}_V] \quad (19)$$

where $\bar{\Sigma}_i, i = S, V, spin$ contain all the parameters of the SUSY models. The modulation is described by the parameter h .

The total directional event rates can be obtained in a similar fashion by suitably modifying Eq. (16)

$$\langle \frac{dR}{du} \rangle_{dir} = \frac{\rho(0)}{m_\chi} \frac{m}{Am_N} \int f(\mathbf{v}, \mathbf{v}_E) \frac{\mathbf{v} \cdot \hat{e} H(\mathbf{v} \cdot \hat{e})}{2\pi} \frac{d\sigma(u, v)}{du} d^3v \quad (20)$$

The role played by the velocity distribution is very clear. What is the proper velocity distribution to use? The best approach seems to be to apply the Eddington approach [53]. In such an approach one starts from a given density as a function of space and one solves Poisson's equation to obtain the potential. Then from the functional dependence of the density on the potential one can construct, at least numerically, the density distribution in phase space, as a function of the potential $\Phi(\mathbf{r})$ and the velocity [53], [41,42,54]. Evaluating this distribution in our vicinity yields the desired velocity distribution. Since this procedure can only be implemented numerically it is very hard to incorporate in the calculation of the directional rates. We thus follow the conventional approach and use two phenomenological velocity distributions: i) A Gaussian distribution, which can be either spherically symmetric or only axially symmetric and ii) A velocity distribution prescribed by the assumption of the late infall in the form of caustic rings.

A. Gaussian Distribution

The Gaussian distribution, with respect to the center of the galaxy, is of the form:

$$f(\mathbf{v}', \lambda) = N(\lambda) \frac{1}{(v_0 \sqrt{\pi})^3} \text{Exp} \left[-\frac{(\lambda + 1)[(v'_y)^2 + (v'_z)^2] + (v'_x)^2}{v_0^2} \right] \quad (21)$$

where v_0 is equal to the velocity of the sun around the center of galaxy, λ is the asymmetry parameter, assumed to be in the range $0 \leq \lambda \leq 1$, and $N(\lambda)$ is a normalization constant, $N(0) = 1$. One must of, course, transform the above distribution into the local coordinate system, taking into account both the motion of the sun as well as that of the Earth. In writing the above velocity distribution we have chosen a set of axes as follows:

The z-axis is along the sun's direction of motion.

The x-axis is the radial direction outwards.

The y- axis is perpendicular to the galactic plane, so that the system is a right-hand one.

Then

$$\mathbf{v}' = \mathbf{v} + v_0 \hat{z} + \mathbf{v}_E, \quad \mathbf{v}_E = v_E [\sin \alpha \hat{x} - \cos \alpha \cos \gamma \hat{y} + \cos \alpha \sin \gamma \hat{z}] \quad (22)$$

with $\gamma \approx \pi/6$ and α the phase of the Earth. After that one must do the folding with the above velocity distribution. The integration, however, of equation 20 is quite difficult due to the presence of the Heavyside function. So for the purpose of integration we found it convenient to go to a coordinate system in which the polar axis is in the direction of observation \hat{e} , which in the above coordinate system is specified by the polar angle Θ and the azimuthal angle Φ . In this new coordinate system polar angle specifying the velocity vector is simply restricted to be $0 \leq \theta \leq \pi$, while the azimuthal angle ϕ is unrestricted. Thus the unit vectors along the new coordinate axes, $\hat{X}, \hat{Y}, \hat{Z}$, are expressed in terms of the old ones as follows:

$$\hat{Z} = \sin \Theta \cos \Phi \hat{x} + \sin \Theta \sin \Phi \hat{y} + \cos \Theta \hat{z}. \quad (23)$$

$$\hat{X} = \cos \Theta \cos \Phi \hat{x} + \cos \Theta \sin \Phi \hat{y} - \sin \Theta \hat{x}. \quad (24)$$

$$\hat{Y} = -\sin \Phi \hat{x} + \cos \Phi \hat{y}. \quad (25)$$

Thus the LSP velocity is expressed in the new coordinate system as:

$$v_x = \sin \Theta \cos \Phi v_X + \sin \Theta \sin \Phi v_Y + \cos \Theta v_Z, \quad (26)$$

$$v_y = \cos \Theta \cos \Phi v_X + \cos \Theta \sin \Phi v_Y - \sin \Theta v_Z, \quad (27)$$

$$v_z = -\sin \Phi v_X + \cos \Phi v_Y, \quad (28)$$

with $v_X = v \sin \theta \cos \phi$, $v_Y = v \sin \theta \sin \phi$, $v_Z = v \cos \theta$. It is thus straightforward to go to polar coordinates in velocity space and get:

$$\left\langle \frac{dR}{du} \right\rangle_{dir} = \frac{\rho(0)}{m_\chi} \frac{m}{Am_N} \int_{av_0\sqrt{u}}^{v_m} v^3 dv \int_0^1 d\xi \int_0^{2\pi} d\phi \frac{\tilde{f}(\Theta, \Phi, v, v_E, \xi, \phi)}{2\pi} \frac{d\sigma(u, v)}{du} \quad (29)$$

with $\xi = \cos \theta$. Now the orientation parameters Θ and Φ appear explicitly in the distribution function and not implicitly via the limits of integration. The function \tilde{f} can be obtained from the velocity distribution, but it will not be explicitly shown here. Thus we obtain:

$$R_{dir} = \bar{R}(t_{dir}/2\pi) [1 + h_m \cos(\alpha - \alpha_m \pi)] \quad (30)$$

where the quantity t_{dir} provides the non modulated amplitude, while h_m describes the modulation amplitude and α_m is the shift in phase (in units of π), giving the phase of the Earth in which the maximum modulation occurs. Clearly these parameters are functions of Θ and Φ as well as the parameters a and Q_{min} . The dependence on a comes from the nuclear form factor the folding with LSP velocity. The other SUSY parameters have all been absorbed in \bar{R} .

Instead of t_{dir} itself it is more convenient to present the reduction factor of the non modulated directional rate compared to the usual non-directional one, i.e.

$$f_{red} = \frac{R_{dir}}{R} = t_{dir}/(2\pi t) = \kappa/(2\pi) \quad (31)$$

It turns out that the parameter κ , being the ratio of two rates, is less dependent on the parameters of the theory. The directional rate can be cast in an even better form as follows:

$$R_{dir} = \bar{R} t \frac{\kappa}{2\pi} [1 + h_m \cos(\alpha - \alpha_m \pi)] \quad (32)$$

Another quantity, which may be of experimental interest is the asymmetry $As = |R_{dir}(-) - R_{dir}(+)|/(R_{dir}(-) + R_{dir}(+))$ in some given direction (+) and its opposite (-). The most relevant direction for the asymmetry is that of the velocity of the sun. As is almost independent of all other parameters except the direction of observation and the velocity distribution. The directional rates exhibit interesting pattern of modulation. From the functions $h_m(a, Q_{min})$ and α_m obtained in the present work, it is trivial to plot the expression (32) as a function of the phase of the earth α . Hence, this will not be done here.

B. Caustic Rings

One would like to examine a non isothermal model to see what effect, if any, may have on the directional rate. The model of caustic rings proposed by Sikivie [55] comes to mind [56], [39]. Admittedly, however, this scenario for dark matter distribution in the galaxy is not broadly accepted [57], since it has not been supported by galaxy evaluation simulations. . From previous work [39] we take the data for caustic rings needed for our purpose , which, for the reader's convenience, we have included in Table I.

The above expressions simplify significantly in the case of caustic rings whereby the velocity distribution is discreet. Thus Eq. (17) takes the form

$$\langle \frac{d\Sigma}{du} \rangle = \frac{2\bar{\rho}}{\rho(0)} a^2 [\bar{\Sigma}_S \bar{F}_0(u) + \frac{\langle v^2 \rangle}{c^2} \bar{\Sigma}_V \bar{F}_1(u) + \bar{\Sigma}_{spin} \bar{F}_{spin}(u)] \quad (33)$$

We remind the reader that $\bar{\rho}$ was obtain for each type of flow (+ or -), which explains the factor of two. in the Sikivie model [55] we have $(2\bar{\rho}/\rho(0)) = 1.25$. The quantities $\bar{F}_0, \bar{F}_1, \bar{F}_{spin}$ are obtained from the corresponding form factors via the equations

$$\bar{F}_k(u) = F^2(u) \bar{\Psi}_k(u) \frac{(1+k)}{2k+1} , \quad k = 0, 1 \quad (34)$$

$$\bar{F}_{spin}(u) = F_{11}(u) \bar{\Psi}_0(u) \quad (35)$$

with

$$\tilde{\Psi}_k(u) = \sqrt{\frac{2}{3}} \sum_{n=1}^N \bar{\rho}_n y_{an}^{2k-1} \Theta\left(\frac{y_{an}^2}{a^2} - u\right) \quad (36)$$

with

$$y_{an} = [(y_{nz} - 1 - \frac{\delta}{2} \sin\gamma \cos\alpha)^2 + (y_{ny} + \frac{\delta}{2} \cos\gamma \cos\alpha)^2 + (y_{nx} - \frac{\delta}{2} \sin\alpha)^2]^{1/2} \quad (37)$$

with $\delta = 2(v_E/\upsilon_0)$. Integrating numerically Eq. (33) we obtain the total undirectional rate as a function of the phase of the Earth. Unlike our previous work we did not make an expansion in terms of δ , in order to better deal with threshold effects. By making a Fourier decomposition of the obtained rate to an accuracy better than 1% we find :

$$R = \bar{R} t \frac{2\bar{\rho}}{\rho(0)} [1 + h(a, Q_{min}) \cos\alpha] \quad (38)$$

In other words the modulation is again described a parameter h , which, of course, takes different numerical values compared to those of the Gaussian distribution. Note that, unlike our earlier work [39], the modulation h in this work is defined with a + sign. So our present value of h in the case of caustic rings is expected to have a phase difference of π compared to that of the usual Gaussian distribution.

Similarly integrating Eq. (20) we get

$$\langle \frac{d\Sigma}{du} \rangle_{dir} = \frac{2\bar{\rho}}{\rho(0)} \frac{a^2}{2\pi} [\bar{\Sigma}_S F_0(u) + \frac{\langle v^2 \rangle}{c^2} \bar{\Sigma}_V F_1(u) + \bar{\Sigma}_{spin} F_{spin}(u)] \quad (39)$$

The quantities F_0, F_1, F_{spin} are obtained from the equations

$$F_k(u) = F^2(u) \Psi_k(u) \frac{(1+k)}{2k+1}, k = 0, 1 \quad (40)$$

$$F_{spin}(u) = F_{11}(u) \Psi_0(u) \quad (41)$$

$$\Psi_k(u) = \sqrt[2k]{\sum_{n=1}^N \bar{\rho}_n y_{an}^{2(k-1)}} X H(X) \quad (42)$$

with $H(X)$ the usual Heaviside (theta) function and X given by

$$X = (y_{nz} - 1 - \frac{\delta}{2} \sin\gamma \cos\alpha) \mathbf{e}_z \cdot \mathbf{e} + (y_{ny} + \frac{\delta}{2} \cos\gamma \cos\alpha) \mathbf{e}_y \cdot \mathbf{e} + (y_{nx} - \frac{\delta}{2} \sin\alpha) \mathbf{e}_x \cdot \mathbf{e} \quad (43)$$

Note that in X only certain rings contribute for a given direction of observation \hat{e} (as dictated by the Heaviside function). Note further that the other Heaviside function for a given ring n restricts the contribution of the form factor as follows:

$$\chi(y_{an}) = \int_{u_{min}}^{y_{an}^2/a^2} F^2(u) du \quad (44)$$

and an analogous expression for the spin response function.

Once again we did not make an expansion in powers of delta. We Fourier decomposed the final expression and we found that Fourier components higher than unity ($n \geq 2$) are negligible. In other words our results for the directional rate can be cast in the form of Eq. (32).

V. RESULTS AND DISCUSSION

The three basic ingredients for the event rate for the LSP-nucleus scattering are the input SUSY parameters, a quark model for the nucleon and the velocity distribution combined with the structure of the nuclei involved. In the present work we will present our results for the coherent scattering and make comparisons with the spin contribution, whenever possible. We will focus our discussion on the light targets (e.g. $A=19, 23, 29$) and the more popular target ^{127}I .

We have utilized two nucleon models indicated by B and C, for their description see our previous work [50], which take into account the presence of heavy quarks in the nucleon. We also considered the effects on the rates of the energy cut off imposed by the detector, by considering two typical cases $Q_{min} = 0, 10 \text{ KeV}$.

The experimentally determined quenching factors, see Simon *et al* and Graichen *et al* [58,59] and references therein, defined as the ratio of a signal induced by nuclear recoil to that of an electron of the same energy, have not been included in calculating the total rates in the present work. These factors, which are functions of the energy, depend mainly on the detector material. For NaI they have been measured [58,60] down to about 10 KeV and they are constant, about 0.25. For our calculations employing $Q_{min} = 10 \text{ KeV}$ this amounts to a reduction of the parameter t to about 25% of its value presented here. We cannot estimate what the effect of quenching is going below

10 KeV. The modulation amplitude and the reduction factor κ , however, being relative parameters, are not expected to be influenced very much by such effects.

A. Isothermal Models

For the reader's convenience we will begin by presenting results for the unmodulated non directional event rates, $\bar{R}t$, of the symmetric isothermal model for a favorable SUSY parameter choice with large $\tan(\beta)$, described previously [20], shown in Fig. 1 as a function of the LSP mass in GeV. Clearly, depending on the SUSY parameter space and in particular the LSP mass, the rates can change many orders of magnitude. What we really want to exhibit is the role of the nucleon model employed and the effect of the energy cutoff.

The two relative parameters, i.e. the quantities t and h , for ^{127}I are shown in Figs 2 and 3 respectively in the case of Gaussian distribution. For the light systems these quantities are essentially constant independent of the LSP mass (the reduced mass does not change as the LSP mass increases). They are shown in Table II. In the case of the directional rates we calculated the reduction factors and the asymmetry parameters as well as the modulation amplitude as functions of the direction of observation, focusing our attention along the three axes [38], i.e along $+z, -z, +y, -y, +x$ and $-x$. In the case of the directional rates we calculated the reduction factors and the asymmetry parameters as well as the modulation amplitude as functions of the direction of observation, focusing our attention along the three axes [38], i.e along $+z, -z, +y, -y, +x$ and $-x$.

Since f_{red} is the ratio of two parameters, its dependence on Q_{min} and the LSP mass is mild. In the case of light nuclear systems ($A=19, 23$ and 29) these parameters are shown in Table II. Note that in the favorable direction $-z$ (opposite to the velocity of the sun) the modulation is about a factor of two bigger than in the non-directional case, but it is still quite small ($h = 0.06$). The reduction factor is $\kappa = 0.7$. In the sun's direction of motion the process is unobservable. In the plane perpendicular in the sun's velocity the rate is further reduced by a factor of about three.

FIGURES

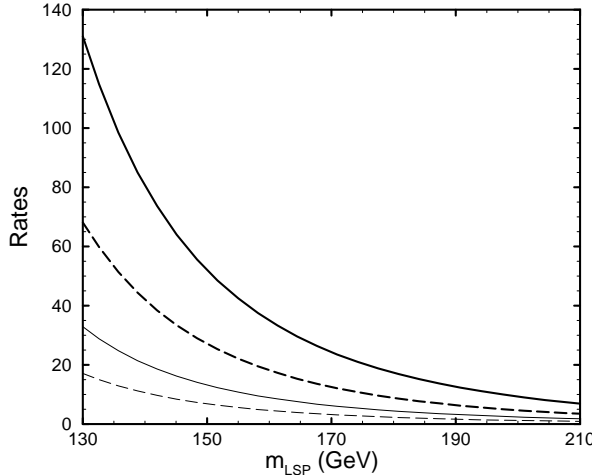


FIG. 1. The Total detection rate per $(kg - target)yr$ vs the LSP mass in GeV for a typical solution of the parameter space, as described in our previous work (see text), in the case of ^{127}I . The results shown by thick lines correspond to model B, while those by a thin line to model C. In the upper curve no detector cutoff was employed, while in the lower curve we used a detector energy cutoff of $Q_{min} = 10$ KeV. Such effects introduce variations in the rates by factors of about two.

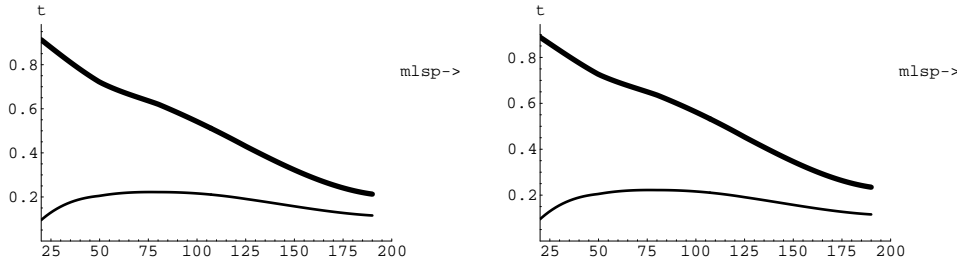


FIG. 2. The dependence of the quantity t on the LSP mass for the symmetric case ($\lambda = 0$) on the left as well as for the maximum axial asymmetry ($\lambda = 1$) on the right in the case of the intermediate mass target ^{127}I . For orientation purposes two detection cutoff energies are exhibited, $Q_{min} = 0$ (thick solid line) and $Q_{min} = 10 \text{ keV}$ (thin solid line). As expected t decreases as the cutoff energy and/or the LSP mass increase. We see that the parameter λ has little effect on the non modulated rate.

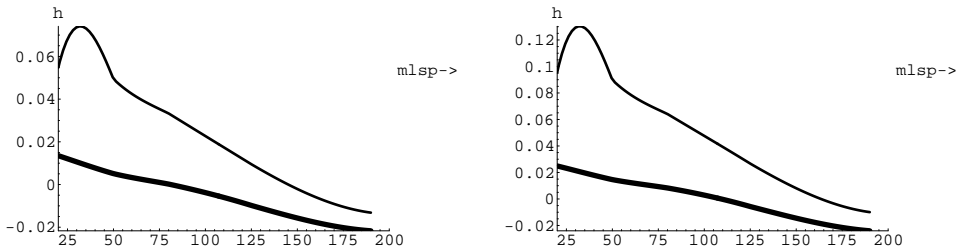


FIG. 3. The same as in Fig. 2 for the modulated amplitude. We see that the modulation is small and decreases with the LSP mass. It even changes sign for large LSP mass. The introduction of a cutoff Q_{min} increases the modulation (at the expense of the total number of counts). It also increases with the parameter λ .

The modulation shows a very interesting pattern. If the observation is done in the direction opposite to the sun's direction of motion, the modulation amplitude h_m behaves in the same way as the non directional one, namely h . It is more instructive to consider directions of observation in the plane perpendicular to the sun's direction of motion ($\Theta = \pi/2$). We see from Table II that now the modulation is quite a bit larger, giving rise to a difference between the maximum and the minimum rates of about 50%.

For heavier nuclei the pattern slightly changes. Our results are presented in plots, in which we adopted the following convention: The thick solid line corresponds to $+z$ ($\Theta = 0$), while the thin line to $-z$ ($\Theta = \pi$). In the case of $\Theta = \pi/2$ we encounter 4 cases. The intermediate thickness line corresponds to the $\pm x$, the dotted line to $+y$ and the dashed line to $-y$. In some cases two or more lines may coincide. In the case of κ one can distinguish only the curves corresponding to the three Θ values.

The quantities κ and h_m show some variation with the LSP mass (see Figs 4 and 6), since in this case the reduced mass changes.

The quantities As and α_m do not show any significant changes compared to those of the light systems (see Fig. 5 and 7. We see that, in the absence of modulation, the asymmetry is non zero only if \hat{e} is in the direction of the sun's motion. In the other directions the asymmetry depends on the phase of the Earth and is the same with the modulation , i.e. $h_m|\cos\alpha|$, $h_m|\sin\alpha|$ in the y-direction (perpendicular in the plane of the galaxy) and x-direction (in the radial direction in the galaxy) respectively.

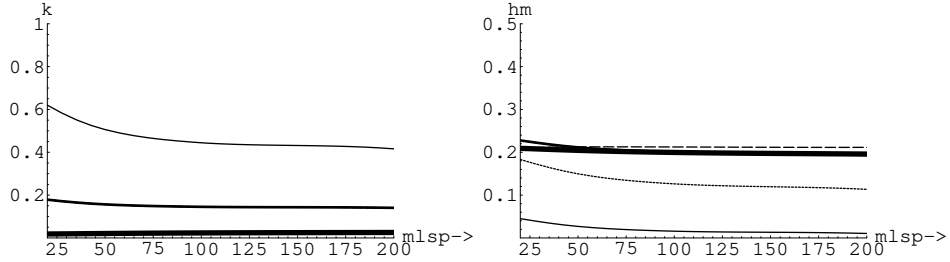


FIG. 4. On the left figure one sees the quantity κ and on the right the quantity h_m for $\lambda = 0$ and $Q_{min} = 0$. The results are almost identical for the coherent and the spin modes. They change very little for $Q_{min} = 10$ KeV. For the identification of the curves see text. Note that in the case of the modulation the curves corresponding to $+z$ and $\pm y$ coincide. The large modulation seen in the $+z$ direction is essentially useless since the event rate is very small.

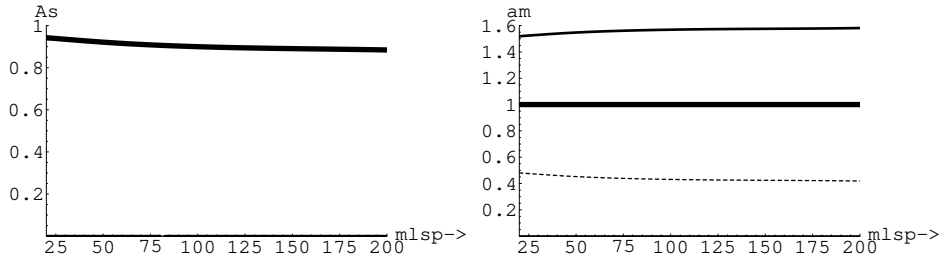


FIG. 5. The quantities As and α_m for $\lambda = 0$ and $Q_{min} = 0$. The asymmetry As , shown on the left, takes only two values $As \approx 1.0$ in the direction of the sun's motion and zero in all other directions. These asymmetry plots do not contain the contribution due to modulation, since, then, the asymmetry would depend on the time of observation (see text). On the right we show the shift (in units of π) in the position of the maximum of the modulated amplitude. This shift is almost zero in the $-z, +y$ directions, close to π in the $+z, -y$ directions, close to $\pi/2$ in the $+x$ direction and almost $3\pi/2$ in the $-x$ direction. The notation is the same as in Fig. (4).

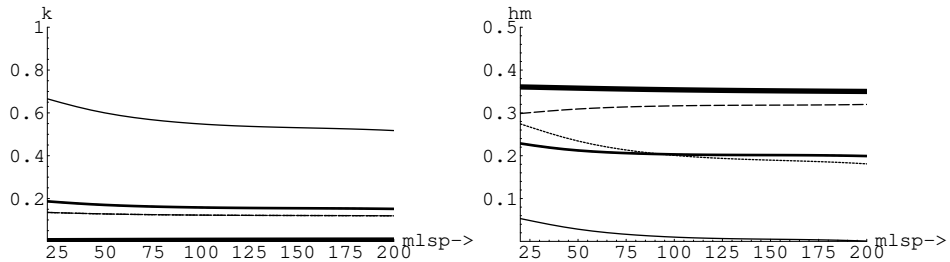


FIG. 6. The same as in Fig. 4 for $\lambda = 1$.

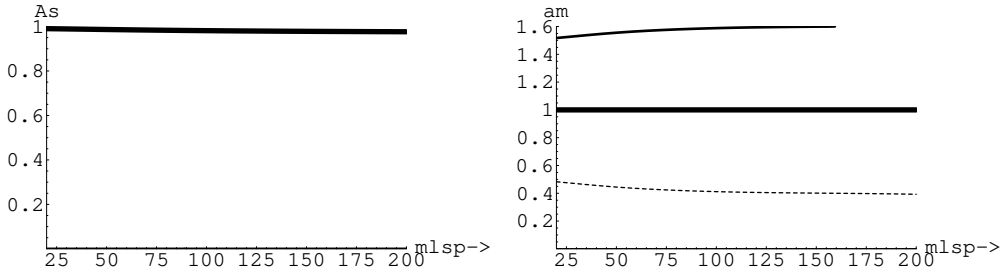


FIG. 7. The same as in Fig. 5 for $\lambda = 1$.

The results for the light systems are presented in Table II.

B. Caustic Rings

The case of non isothermal models, e.g. caustic rings, has previously been discussed [39] in some special cases. Here we will expand our discussion further. In the case of the non directional rates, the quantities t and h for ^{127}I are shown in Figs 8. We see that as far as t is concerned there is no essential difference between caustic rings and Gaussian distribution. Notice, however, that the modulation is now smaller and of opposite sign. In the case of directional rates the quantities κ and h_m for ^{127}I are shown in Figs 9 and 10 for $Q_{min} = 0, 10 \text{ KeV}$ respectively. The results obtained for the light systems are shown in Table III. One clearly sees that the maximum rate is now in the direction of the sun's motion, $+z$, and the minimum in the $-z$ direction, i.e. in the opposite sense compared with the Gaussian distribution. In the other directions the rates fall in between. Naturally the rate is reduced in the presence of an energy cutoff, but in the case of caustic rings the reduction manifests itself mainly for small LSP masses. For such masses it is not easy to have energy above threshold transferred to the nucleus motion, but smaller than in the Gaussian distribution ($As = 0.75$ and $As = 0.68$ for $Q_{min} = 0$ and 10 KeV respectively). In the other directions the asymmetry is governed by the modulation.

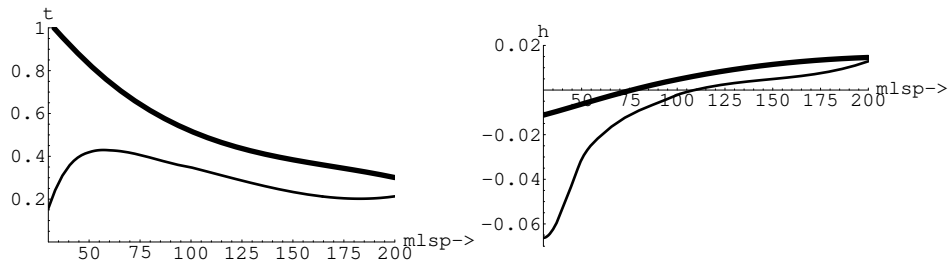


FIG. 8. The same as in Fig. 2 (left figure) and 3 (right figure) in the case of caustic rings.

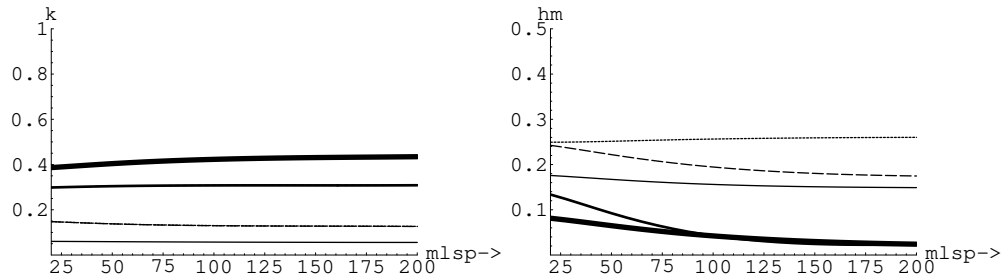


FIG. 9. The same as in Fig. 4 for caustic rings with $Q_{min} = 0$ (λ is irrelevant).

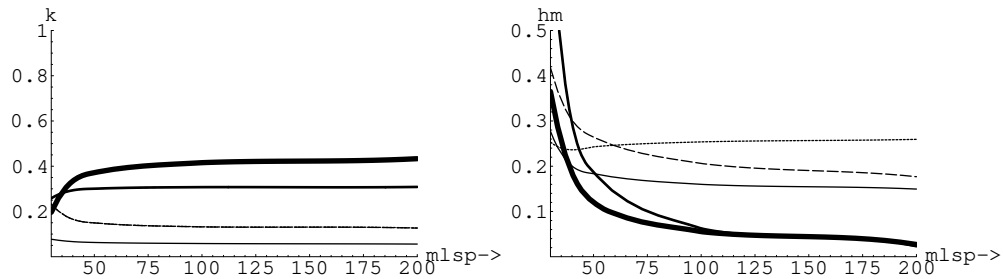


FIG. 10. The same as in Fig. 9 for caustic rings with $Q_{min} = 10$.

VI. CONCLUSIONS

In the present paper we have discussed the parameters, which describe the event rates for direct detection of SUSY dark matter. Only in a small segment of the allowed parameter space the rates are above the present experimental goals [20,22,24]. We thus looked for characteristic experimental signatures for background reduction, i.e. a) Correlation of the event rates with the motion of the Earth (modulation effect) and b) the directional rates (their correlation both with the velocity of the sun and that of the Earth.)

A typical graph for the total non modulated rate is shown Fig. 1. The relative parameters t and h in the case of non directional experiments are exhibited in Fig. 2 and Fig. 3 for the Gaussian models. For caustic rings they are shown in Fig. 8. We must emphasize that the two graphs of Figs. 2 and 8 do not contain the entire dependence on the LSP mass. This is due to the fact that there is the extra factor m_χ^{-1} in Eq. (19) and a factor of μ_r^2 arising from Σ_i , $i = S, \text{spin}, V$ (see Eqs (6), (7), and (10)). All these factors combined lead to a essentially a constant. There remains, however, an LSP mass dependence, which is due to the fact that the nucleon cross section itself dramatically depends on the LSP mass.

Figs 2, 3 and 8 were obtained for the scalar interaction, but similar behavior is expected for the spin contribution. From the point of view of the static spin matrix elements the most favored system is the $A = 19$ (see our previous work [33]). The scale of the total spin contribution, coming from the SUSY dependent parameter $\bar{\Sigma}_s$, which was not discussed in this work, may be very very different from the corresponding to the scalar amplitude quantity. We should also mention that in the non directional experiments the modulation $2h$ is small, i.e. for $\lambda = 0$ less than 4% for $Q_{min} = 0$ and increases to 12% for $Q_{min} = 10 \text{ KeV}$ (at the expense of the total number of counts). For $\lambda = 1$ there is no change for $Q_{min} = 0$, but it can go as high as 24% for $Q_{min} = 10 \text{ KeV}$. In the case of caustic rings is smaller and of opposite sign.

For the directional rates it is instructive to examine the reduction factors κ if the observation is made in a specific direction, e.g. along the three axes, i.e along $+z, -z, +y, -y, +x$ and $-x$. These depend on the nuclear parameters, the reduced mass,

the energy cutoff Q_{min} and λ [38]. Since f_{red} is the ratio of two parameters, its dependence on Q_{min} and the LSP mass is mild. So we present results for ^{127}I in Figs 4 and 6 (see also Figs 9 and 10 for caustic rings). In the case of light systems our results are presented in Tables II and III. As expected the maximum rate is along the sun's direction of motion, i.e opposite to its velocity ($-z$) in the Gaussian distribution and $+z$ in the case of caustic rings. In fact we find that $\kappa(-z)$ is around 0.5 ($\lambda = 0$) and around 0.6 ($\lambda = 1.0$). It is not very different from the naively expected $f_{red} = 1/(2\pi)$, $\kappa = 1$. The asymmetry along the sun's direction of motion, $As = |R_{dir}(-) - R_{dir}(+)|/(R_{dir}(-) + R_{dir}(+))$ is quite characteristic, i.e. almost unity for Gaussian models and a bit smaller in the case of caustic rings. The rate in the other directions is quite a bit smaller (see Tables II and III) and the asymmetry is equal to the absolute value of the modulation.

The disadvantage of smaller rates in the plane perpendicular to the sun's velocity may be compensated by the bonus of very large and characteristic modulation.

In conclusion: in the case of directional non modulated rates we expect unambiguous correlation with the motion on the sun, which can be explored by the experimentalists. If one concentrates in a given direction there appears a reduction factor. The reduction factor in the most favored direction, i.e in the line of the motion of the sun, is approximately only $1/(4\pi)$ relative to the non directional experiments. In the plane perpendicular to the motion of the sun we expect interesting modulation signals, but the reduction factor becomes worse. These reduction factors do not appear to be an obstacle to the experiments, since the TPC counters to be used in the planned experiments can make observations in almost all directions simultaneously [61]. Once some candidate events are seen, one can analyze them further in the way we propose here by selecting those corresponding to a given direction of observation.

This work was supported by the European Union under the contracts RTN No HPRN-CT-2000-00148 and TMR No. ERBFMRX-CT96-0090. During the last stages of this work the author was in Tuebingen as a Humboldt awardee. He is indebted to professor Faessler for hospitality and to the Alexander von Humboldt Foundation for its support.

REFERENCES

- [1] S. Hanany *et al*, *Astrophys. J.* **545**, L5 (2000);
 J.H.P Wu *et al*, *Phys. Rev. Lett.* **87**, 251303 (2001);
 M.G. Santos *et al*, *Phys. Rev. Lett.* **88**, 241302 (2002)
- [2] P.D. Mauskopf *et al*, *Astrophys. J.* **536**, L59 (20002);
 S. Mosi *et al*, *Prog. Nuc.Part. Phys.* **48**, 243 (2002);
 S.B. Ruhl *et al*, astro-ph/0212229 and references therein.
- [3] N.W. Halverson *et al*, *Astrophys. J.* **568**, 38 (2002)
 L.S. Sievers *et al*, astro-ph/0205287 and references therin.
- [4] G.F. Smoot *et al*, (COBE data), *Astrophys. J.* **396**, (1992) L1.
- [5] A.H. Jaffe *et al*, *Phys. Rev. Lett.* **86**, 3475 (2001).
- [6] E. Gawiser and J. Silk, *Science* **280**, 1405 (1988); M.A.K Gross, R.S. Somerville, J.R. Primack, J. Holtzman and A.A. Klypin, *Mon. Not. R. Astron. Soc.* **301**, 81 (1998).
- [7] A.G. Riess *et al*, *Astron. J.* **116**, 1009 (1998).
- [8] R.S. Somerville, J.R. Primack and S.M. Faber, astro-ph/9806228; *Mon. Not. R. Astron. Soc.* (in press).
- [9] S. Perlmutter *et al* *Astrophys. J.* **517**, 565 (1997); **483**, 565 (1999); *astro-ph/9812133*.
 S. Perlmutter, M.S. Turner and M. White, *Phys. Rev. Lett.* **83**, 670 (1999).
- [10] J.R. Primack, astro-ph/0205391
- [11] Jaan Einasto, in Dark Matter in Astro- and Particle Physics, p.3, Ed. H.V. Klapdor-Kleingrothaus, Springer-Verlag Berlin Heidelberg 2001.
- [12] D.P. Bennett *et al.*, (MACHO collaboration), A binary lensing event toward the LMC: Observations and Dark Matter Implications, Proc. 5th Annual Maryland Conference, edited by S. Holt (1995);
 C. Alcock *et al.*, (MACHO collaboration), *Phys. Rev. Lett.* **74**, 2967 (1995).

[13] R. Bernabei et al., INFN/AE-98/34, (1998); R. Bernabei et al., *it Phys. Lett. B* **389**, 757 (1996).

[14] R. Bernabei et al., *Phys. Lett. B* **424**, 195 (1998); **B 450**, 448 (1999).

[15] M.W. Goodman and E. Witten, *Phys. Rev. D* **31**, 3059 (1985).

[16] K. Griest, *Phys. Rev. Lett* **61**, 666 (1988).

[17] J. Ellis, and R.A. Flores, *Phys. Lett. B* **263**, 259 (1991); *Phys. Lett. B* **300**, 175 (1993); *Nucl. Phys. B* **400**, 25 (1993).

[18] J. Ellis and L. Roszkowski, *Phys. Lett. B* **283**, 252 (1992).

[19] For more references see e.g. our previous report:
 J.D. Vergados, Supersymmetric Dark Matter Detection- The Directional Rate and the Modulation Effect, hep-ph/0010151;

[20] M.E. Gómez and J.D. Vergados, *Phys. Lett. B* **512**, 252 (2001); hep-ph/0012020.
 M.E. Gómez, G. Lazarides and Pallis, C., *Phys. Rev. D* **61** (2000) 123512 and *Phys. Lett. B* **487**, 313 (2000).

[21] M.E. Gómez and J.D. Vergados, hep-ph/0105115.

[22] A. Bottino *et al.*, *Phys. Lett B* **402**, 113 (1997).
 R. Arnowitt. and P. Nath, *Phys. Rev. Lett.* **74**, 4952 (1995); *Phys. Rev. D* **54**, 2394 (1996); hep-ph/9902237;
 V.A. Bednyakov, H.V. Klapdor-Kleingrothaus and S.G. Kovalenko, *Phys. Lett. B* **329**, 5 (1994).

[23] J.D. Vergados, *J. of Phys. G* **22**, 253 (1996).

[24] A. Arnowitt and B. Dutta, Supersymmetry and Dark Matter, hep-ph/0204187.

[25] E. Accomando, A. Arnowitt and B. Dutta, Dark Matter, muon G-2 and other accelerator constraints, hep-ph/0211417.

[26] T.S. Kosmas and J.D. Vergados, *Phys. Rev. D* **55**, 1752 (1997).

- [27] M. Drees and N.M. Nojiri, *Phys. Rev. D* **47** (1993) 376; (1985).
- [28] M. Drees and N.N. Nojiri, *Phys. Rev. D* **48**, 3843 (1993); *Phys. Rev. D* **47**, 4226 (1993).
- [29] A. Djouadi and MK. Drees, *Phys. Lett. B* **484**, 183 (2000); S. Dawson, *Nucl. Phys. B* **359**, 283 (1991); M. Spira et al, *Nucl. Phys. B* **453**, 17 (1995).
- [30] T.P. Cheng, *Phys. Rev. D* **38**, 2869 (1988); H-Y. Cheng, *Phys. Lett. B* **219**, 347 (1989).
- [31] M.T. Ressell et al., *Phys. Rev. D* **48**, 5519 (1993);
- [32] J.D. Vergados and T.S. Kosmas, *Physics of Atomic nuclei*, Vol. **61**, No 7, 1066 (1998) (from *Yadernaya Fisika*, Vol. 61, No 7, 1166 (1998)).
- [33] P.C. Divari, T.S. Kosmas, J.D. Vergados and L.D. Skouras, *Phys. Rev. C* **61** (2000), 044612-1.
- [34] A.K. Drukier, K. Freese and D.N. Spergel, *Phys. Rev. D* **33**, 3495 (1986).
- [35] K. Freese, J.A Friedman, and A. Gould, *Phys. Rev. D* **37**, 3388 (1988).
- [36] J.D. Vergados, *Phys. Rev. D* **58**, 103001-1 (1998).
- [37] J.D. Vergados, *Phys. Rev. Lett* **83**, 3597 (1999).
- [38] J.D. Vergados, *Phys. Rev. D* **62**, 023519 (2000).
- [39] J.D. Vergados, *Phys. Rev. D* **63**, 06351 (2001).
- [40] J.I. Collar et al, *Phys. Lett. B* **275**, 181 (1992).
- [41] P. Ullio and M. Kamiokowski, *JHEP* **0103**, 049 (2001).
- [42] P. Belli, R. Cerulli, N. Fornego and S. Scopel, *Phys. Rev. D* **66**, 043503 (2002); hep-ph/0203242.
- [43] A. Green, *Phys. Rev. D* **66**, 083003 (2002)
- [44] K.N. Buckland, M.J. Lehner and G.E. Masek, in Proc. *3nd Int. Conf. on Dark Matter*

in Astro- and part. Phys. (Dark2000), Ed. H.V. Klapdor-Kleingrothaus, Springer Verlag (2000).

[45] *CDF Collaboration*, FERMILAB-Conf-99/263-E CDF;
<http://fnalpubs.fnal.gov/archive/1999/conf/Conf-99-263-E.html>.

[46] P.J. Dorman *ALEPH Collaboration* March 2000,
<http://alephwww.cern.ch/ALPUB/seminar/lepcmar200/lepc2000.pdf>.

[47] L3 collabtation, M. Acciari *et al*, *Phys. Lett. B* **495**, 18 (2000); hep-ex/0011043
ALEPH collabtation, R. Barate *et al*, *Phys. Lett. B* **495**, 1 (2000); hep-ex/0011045
DELPHI collabtation, P. Abreu *et al*, *Phys. Lett. B* **499**, 23 (2001)
OPAL collabtation, G. Abbiendi *et al*, *Phys. Lett. B* **499**, 38 (2000).

[48] A. Bottino, N. Fornengo and S. Scopel, *Nucl. Phys. B* **608**, 461 (2001); hep-ph/0212379.

[49] S. Ambrosanio, A. Dedes, S. Heinemeyer, S. Su, and G. Weiglein, *Nuc. Phys. B* **624**, 3 (2002); hep-ph/0106255.

[50] J.D. Vergados, SUSY Dark Matter in Universe- Theoretical Direct Detection Rates, Proc. *NANP-01, International Conference on Non Accelerator New Physics*, Dubna, Russia, June 19-23, 2001, Editors V. Bednyakov and S. Kovalenko, hep-ph/0201014.

[51] A. Bottino, F. Donato, N. Forengo and S. Scopel *Phys. Rev. D* **59**, 095004 (1999).

[52] E. Accomendo, R. Arnowitt, B. Dutta and Y. Santoso, *Nuc. Phys. B* **585**, 124 (2000).

[53] A.S. Eddington *NRAS* **76**, 572 (1916);
D. Merrit, *A J* **90**, (1985)

[54] J.D. Vergados and D. Owen, to appear in *ApJ*, astro-ph/0203293

[55] P. Sikivie, I. Tkachev and Y. Wang, *Phys. Rev. Lett.* **75**, 2911 (1995); *Phys. Rev. D* **56**, 1863 (1997); *Phys. Rev. D* **60**, 063501 (1999)
P.Sikivie, *Phys. Lett. B* **432**, 139 (1998); astro-ph/0109296,astro-ph/9810286

[56] G. Gelmini and P. Gondolo, *Phys. Rev. D* **64**, 023504 (2001)

- [57] B. Moore *et al*, *Phys. Rev. D* **64**, 063508 (2001);
 B. Moore, IDM 2000, 3nd Workshop on the Ident. of Dark Matter, Ed. N. Spooner,
 World Scientific, astro-ph/0103094
 A. Helmi, S.D.M. White and V. Springer, *Phys. Rev. D* **66**, 063502, astro-ph/0201289
- [58] E. Simon *et al*, SICANE:A detector Array for the Measurement of Nuclear Recoil Quenching Factors using a Monoenergetic Neutron Beam, astro-ph/0212491.
- [59] J. Graichen *et al*, *Nucl. Instr. Meth. A* **485**, 774 (2002).
- [60] G. Gerbier *et al*, **Astropart. Phys.** **11**, 287 (1999);
 D.R. Tovey *et al*, *Phys. Lett. B* **433**, 150 (1998);
 J.J.C. Spooner *et al*, *Phys. Lett. B* **321**, 156 (1994).
- [61] Y. Giomataris, Ph. Rebougeant, J.P. Robert and C. Charpak, *Nucl. Instr. Meth A* bf 376, 29 (1996);
 J.I. Collar, Y. Giomataris, Low background applications of Micromegas detector technology, Presented at *IMAGING 2000*, Stockholm 28.06.2000-01.07.2000, DAPNIA/00-08;
 J. Bouchez and Y. Giomataris, Private communication.

TABLES

TABLE I. The quantities $a_n, yi'_n = v_n/v_0, y_{nz} = v_{n\phi}/v_0, y_{ny} = v_{nz}/v_0, y_{nx} = v_{nr}/v_0$ and $\bar{\rho}_n = d_n/[\sum_{n=1}^{20} d_n]$ and $y_n = [(y_{nz} - 1)^2 + y_{ny}^2 + y_{nx}^2]^{1/2}$ (for the other definitions see text).

| n | $a_n(Kpc)$ | y_n' | y_{nz} | y_{ny} | y_{nx} | y_n | $\bar{\rho}_n$ |
|----|------------|--------|----------|-------------|-------------|-------|----------------|
| 1 | 38.0 | 2.818 | 0.636 | ± 2.750 | 0.000 | 2.773 | 0.0120 |
| 2 | 19.0 | 2.568 | 1.159 | ± 2.295 | 0.000 | 2.301 | 0.0301 |
| 3 | 13.0 | 2.409 | 1.591 | ± 1.773 | 0.000 | 1.869 | 0.0601 |
| 4 | 9.7 | 2.273 | 2.000 | ± 1.091 | 0.000 | 1.480 | 0.1895 |
| 5 | 7.8 | 2.182 | 2.000 | 0.000 | ± 0.863 | 1.321 | 0.2767 |
| 6 | 6.5 | 2.091 | 1.614 | 0.000 | ± 1.341 | 1.475 | 0.0872 |
| 7 | 5.6 | 2.023 | 1.318 | 0.000 | ± 1.500 | 1.533 | 0.0571 |
| 8 | 4.9 | 1.955 | 1.136 | 0.000 | ± 1.591 | 1.597 | 0.0421 |
| 9 | 4.4 | 1.886 | 0.977 | 0.000 | ± 1.614 | 1.614 | 0.0331 |
| 10 | 4.0 | 1.818 | 0.864 | 0.000 | ± 1.614 | 1.619 | 0.0300 |
| 11 | 3.6 | 1.723 | 0.773 | 0.000 | ± 1.614 | 1.630 | 0.0271 |
| 12 | 3.3 | 1.723 | 0.682 | 0.000 | ± 1.591 | 1.622 | 0.0241 |
| 13 | 3.1 | 1.619 | 0.614 | 0.000 | ± 1.568 | 1.615 | 0.0211 |
| 14 | 2.9 | 1.636 | 0.545 | 0.000 | ± 1.545 | 1.611 | 0.0180 |
| 15 | 2.7 | 1.591 | 0.500 | 0.000 | ± 1.500 | 1.581 | 0.0180 |
| 16 | 2.5 | 1.545 | 0.454 | 0.000 | ± 1.477 | 1.575 | 0.0165 |
| 17 | 2.4 | 1.500 | 0.409 | 0.000 | ± 1.454 | 1.570 | 0.0150 |
| 18 | 2.2 | 1.455 | 0.386 | 0.000 | ± 1.409 | 1.537 | 0.0150 |
| 19 | 2.1 | 1.432 | 0.364 | 0.000 | ± 1.386 | 1.525 | 0.0135 |
| 20 | 2.0 | 1.409 | 0.341 | 0.000 | ± 1.364 | 1.515 | 0.0135 |

TABLE II. The quantities κ, h_m, α_m and As for the light nuclear systems ($A=19, 23$ and 29), are almost identical. The difference between the coherent and the spin mode is less than 1%. They are also essentially independent of the LSP mass and the SUSY parameters. Note the phase of the modulation in the directions $-z$, $+y$ is the same as in the non directional case. The phase of the modulation in the $-y$ direction is reversed (minimum in June 3nd). The phase in the $\pm x$ directions leads to a maximum in between. When the range of a variable is given, it depends somewhat on the LSP mass (the mass increases to the right).

| quantity | dir | $\lambda = 0$ | $\lambda = 0$ | $\lambda = 1.0$ | $\lambda = 1.0$ |
|------------|-----|---------------------|------------------------------|---------------------|------------------------------|
| | | $Q_{min} = 0.0$ | $Q_{min} = 10.0 \text{ KeV}$ | $Q_{min} = 0.0$ | $Q_{min} = 10.0 \text{ KeV}$ |
| t | all | 1.0 | 0.6 | 1.0 | 0.6 |
| h | all | 0.02 | 0.04-0.06 | 0.04 | 0.05-0.08 |
| | +z | 0.018 | 0.010 | 0.003 | 0.000 |
| | x | 0.190 | 0.177 | 0.211 | 0.145 - 0.186 |
| κ | y | 0.190 | 0.177 - 0.180 | 0.150 | 0.087 - 0.125 |
| | -z | 0.690 | 0.758 - 0.760 | 0.752 | 0.519 - 0.672 |
| | +z | 0.211 | 0.242 - 0.226 | 0.361 | 0.380 |
| | +x | 0.235 | 0.292 - 0.255 | 0.237 | 0.325 - 0.261 |
| | +y | 0.199 | 0.299 - 0.233 | 0.290 | 0.456 - 0.347 |
| h_m | -x | 0.235 | 0.292 - 0.255 | 0.237 | 0.325 - 0.261 |
| | -y | 0.199 | 0.199 - 0.208 | 0.290 | 0.243 - 0.280 |
| | -z | 0.060 | 0.100 - 0.068 | 0.063 | 0.158 - 0.092 |
| | +z | 1 | 1 | 1 | 1 |
| | +x | 1/2 | 0.445 - 0.484 | 1/2 | 0.432 - 0.467 |
| | +y | 0 | 0 | 0 | 0 |
| α_m | -x | 3/2 | 1.555 - 1.586 | 3/2 | 1.587 - 1.533 |
| | -y | 1 | 1 | 1 | 1 |
| | -z | 0 | 0 | 0 | 0 |
| | z | 0.945 | 0.989 - 0.970 | 0.991 | 1.000 |
| As | x | $h_m \sin \alpha $ | $h_m \sin \alpha $ | $h_m \sin \alpha $ | $h_m \sin \alpha $ |
| As | y | $h_m \cos \alpha $ | $h_m \cos \alpha $ | $h_m \cos \alpha $ | $h_m \cos \alpha $ |

TABLE III. The same as in Table II in the case of caustic rings for for the light nuclear systems ($A=19, 23$ and 29). Note the difference in the phases between the modulations of the two tables.

| quantity | dir | coherent | coherent | spin | spin |
|------------|-----|---------------------|------------------------------|---------------------|------------------------------|
| | | $Q_{min} = 0.0$ | $Q_{min} = 10.0 \text{ KeV}$ | $Q_{min} = 0.0$ | $Q_{min} = 10.0 \text{ KeV}$ |
| t | all | 1.23 - 1.20 | 0.547 - 0.893 | 1.29 - 1.14 | 0.520 - 0.845 |
| h | all | -0.015 | -0.057 - (-0.026) | - 0.015 | -0.057 - (-0.025) |
| | +z | 0.381 | 0.310 - 0.364 | 0.383 | 0.310 - 0.363 |
| | x | 0.297 | 0.281 - 0.293 | 0.297 | 0.281 - 0.293 |
| κ | y | 0.150 | 0.182 - 0.159 | 0.149 | 0.183 - 0.159 |
| | -z | 0.060 | 0.067 - 0.062 | 0.060 | 0.068 - 0.062 |
| | +z | 0.086 | 0.208 - 0.112 | 0.083 | 0.310 - 0.113 |
| | +x | 0.143 | 0.351 - 0.195 | 0.139 | 0.351 - 0.195 |
| | +y | 0.249 | 0.239 - 0.246 | 0.249 | 0.239 - 0.246 |
| h_m | -x | 0.144 | 0.351 - 0.195 | 0.137 | 0.351 - 0.195 |
| | -y | 0.247 | 0.315 - 0.267 | 0.245 | 0.281 - 0.267 |
| | -z | 0.178 | 0.209 - 0.187 | 0.178 | 0.209 - 0.187 |
| | +z | 1 | 1 | 1 | 1 |
| | +x | 3/2 | 3/2 | 3/2 | 3/2 |
| | +y | 0 | 0 | 0 | 0 |
| α_m | -x | 1/2 | 1/2 | 1/2 | 1/2 |
| | -y | 1 | 1 | 1 | 1 |
| | -z | 0 | 0 | 0 | 0 |
| | z | 0.726 | 0.667 | 0.728 | 0.667 |
| As | x | $h_m \sin \alpha $ | $h_m \sin \alpha $ | $h_m \sin \alpha $ | $h_m \sin \alpha $ |
| As | y | $h_m \cos \alpha $ | $h_m \cos \alpha $ | $h_m \cos \alpha $ | $h_m \cos \alpha $ |

amHm1spL

